University of Thi-Qar Journal of Science (UTJsci)
E-ISSN: 2709-0256, P-ISSN: 1991-8690, Vol. 11, No. 1, Jun. 2024

# Effect of Saturable Absorber Length on Characteristics of Dual Laser Pulses of Passive Q-Switched

Sara Abdulhussain *[1a] , Abdul-Kareem Mahdi Salih [2b] and Rasool Asal [3c]

[1] College of Engineering, University of Thi-Qar, Thi-Qar, Iraq.
[2] Department of Physics, College of Science, University of Thi-Qar, Thi-Qar, Iraq.
[3] Sesar Lab,University of Milan,Italy .
[b] E-mail: karimmahdisalih@yahoo.co.uk , [c] E-mail: rraa5085@gmail.com
[a*]Corresponding author: Sarah2017711@gmail.com

Received: 2023-12-17, Revised: 2024-01-21, Accepted: 2024-01-24, Published: 2024-06-01

***Abstract*— The effect of saturable absorber material length on the characteristics of the dual passive Q-switching pulses generated from two wavelengths ( $\lambda = 0.946\,\mu m$) and $\lambda = 1.064\,\mu m$) instead of single wavelength was simulated. Numerical solution of our previous rate equations model using Rung-Kutta-Fahelberg method has been utilized in simulation. $Nd^{+3}$ :YAG using as an active medium, and $Cr^{+4}$:YAG as a saturable absorber material. The results showed that the $Nd^{+3}$:YAG dual passive Q-switching generated or released at an advanced(earlier) time and characterized by short duration times, high energy and high power with the increasing in the value of $L_{sa}$. The passive Q-switching for $\lambda = 1.064\,\mu m$ , $\lambda = 0.946\,\mu m$) are released respectively at time 58ns, 60 ns approximately at $L_{sa} = 0.35cm$ , while released at time 34 ns, 36 ns respectively approximately at $L_{sa} = 0.46cm$ . The duration time of $\lambda = 1.064nm$ , $\lambda = 0.946nm$ pulses approximate to 16.8ns, 14.6 ns respectively at $L_{sa} = 0.35cm$ , while approximate to 10.8 ns ,9.2 ns respectively at $L_{sa} = 0.46cm$ .**

***Keywords*—Laser, high Power Pulses, Passive Q-switching, solid-state laser**

## I. INTRODUCTION

Passive Q-switched is one type of Q-switched techniques that were used to compress the laser energy to a narrow pulse to improve the power of the output laser pulses [1,2] . It relies on optical element called saturable absorber material (SA). There are many practical applications of the pulses generated by this technique such as biomedicine, precision measurement, spectroscopy, medical treatment, lidars, material processing, nonlinear optics, and range finders [3-4]. The development of lasers has always been conditioned by the availability of suitable materials for their uses $Cr^{+4}$:YAG saturable absorber material is very suitable for working with $Nd^{+3}$:YAG as active medium (AM) in passive Q-switched optical system [2,4]. The optical system that was simulated in this study included $Cr^{+4}$:YAG and $Nd^{+3}$:YAG as a SA and AM, respectively.

The optical dynamics of $Cr^{+4}$:YAG are usually described by a four-level model, as shown in Figure 1 [5], The four-level system has three parameters: recovery time of the excited state $\tau$, ground-state absorption cross section $\sigma_{gs}$, and excited-state absorption cross section $\sigma_{es}$. The influence of pump photons causes the ions to move from the ground state to the excites state ($E_3$) by absorption process depending on the ground-state absorption cross section ( $\sigma_{gs}$). The excites state ($E_3$) characterizes by short lifetime $\tau$ which causes the fast decay to the excites state ($E_2$) Also, due to the process of absorption depends on the excite -state absorption cross section ($\sigma_{es}$) the ions move from the $E_2$ state to the excites state ($E_4$) and returns by very fast decay to $E_2$ state due to the very short lifetime of $E_4$ state. Moreover the optical dynamics of $Cr^{+4}$:YAG depends mainly on the states $E_1$ and $E_3$ [5,6]. Figure 2 [2,7] shows the diagram of energy level of $Nd^{+3}$: YAG, $Nd^{+3}$-doped crystals. It is one of the most studied lanthanide ions in glass because of its important spectrum. It represents by the transition from $^4F_{3/2}$ to $^4I_{9/2}$ . It also represents three or quasi three-level laser system of AM. The lowest laser level is the uppermost component of the five crystal-feld components of the ground-state $^4I_{9/2}$ level. This transition gives emission spectrum near $\lambda = 0.946\,\mu m$ . The second important spectrum results from the transition between $^4F_{3/2}$ and $^4I_{11/2}$ , and it represents four level schemes of AM that gives emission spectrum near 1.064um. The three-level laser system is different optical mechanism from the traditional four-level and three-level laser systems. The absorption spectrum of SA $Cr^{+4}$:YAG is in a good suitable with both emission spectrum of $Nd^{+3}$:YAG[8-10].

In previous study [11], the rate equation model was formulated mathematically to simulate the laser system optical performance by employing the two type spectra of $Nd^{+3}$:YAG ($\lambda = 0.946\,\mu m$ and $\lambda = 1.064\,\mu m$ ). In this stud, we employ the mathematical model to simulate the effect of SA length on the characteristics of the dual passive Q-

This work is licensed under a Creative Commons Attribution 4.0 International License.
https://doi.org/10.32792/utq/utjsci/v11i1.1151

switching pulses generated from two wavelengths YAG ( $\lambda = 0.946\,\mu m$ and $\lambda = 1.064\,\mu m$ ) instead of single wavelength.

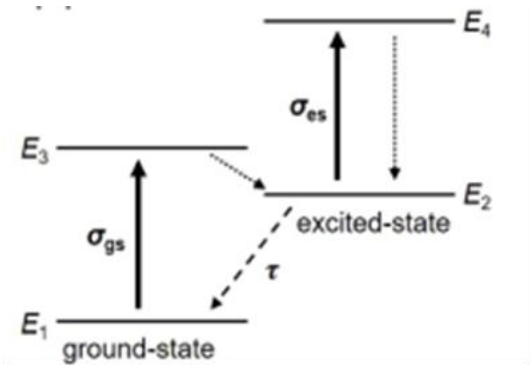


Figure 1: Energy-level scheme of $Cr^{+4}$: YAG [5].

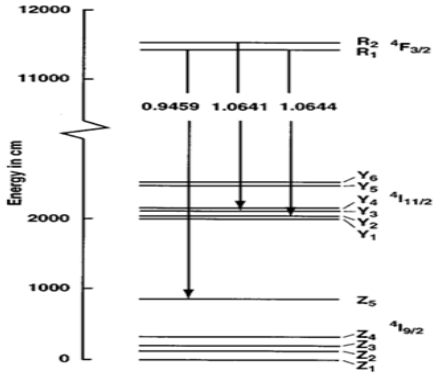


Figure 2: Energy-level diagram of Nd:YAG [2,7]

## II. THEORY

The rate equations model as the following [11] were used in the simulation:

$$\frac{d\varphi_1}{dt} = \varphi_1\left[K_{am1}N_{g1} - K_{sg1}n_{sg} - K_{se1}n_{se} - \gamma_{c1}\right] \quad (1)$$

$$\frac{d\varphi_2}{dt} = \varphi_2\left[K_{am2}N_{g2} - K_{sg2}n_{sg} - K_{se2}n_{se} - \gamma_{c2}\right] \quad (2)$$

$$\frac{dN_{g1}}{dt} = R_p - \gamma_{p1}K_{am1}N_{g1}\varphi_1 - \frac{N_{g1}}{\tau_g} \quad (3)$$

$$\frac{dN_{g2}}{dt} = R_p - \gamma_{p2}K_{am2}N_{g2}\varphi_2 - \quad (4)$$

$$\frac{dn_{sg}}{dt} = -K_{sg1}n_{sg}\varphi_1 - K_{sg2}n_{sg}\varphi_2 + \frac{n_{se}}{\tau_{se}} \quad (5)$$

$$\frac{dn_{se}}{dt} = K_{sg1}n_{sg}\varphi_1 + K_{sg2}n_{sg}\varphi_2 - \frac{n_{se}}{\tau_{se}} \quad (6)$$

where $\varphi_1, \varphi_2$ are the photon densities ($cm^{-3}$) of PQS pulses which are generated from $\lambda_1$, $\lambda_2$ laser respectively ($\varphi_1$ belong to 4-level scheme, while $\varphi_2$ is belong to 3-level scheme). $N_{g1}$ is the population inversion density (PID) of ions ($cm^{-3}$) between $^4F_{3/2}$ and $^4F_{11/2}$ spectrum lines. $N_{g2}$ is the PID of ions between $^4F_{3/2}$ and $^4F_{9/2}$ spectrum lines. $K_{ami(i=1,2)} = \frac{2\sigma_{ai}l_{am}}{\tau_r}$ is the coupling coefficient between the $\varphi_1$ , $\varphi_2$ photons and the ions of excited level of AM ( $^4F_{3/2}$ ). $\sigma_{ai}$ is the emission cross section ($cm^2$) of AM at 4-energy level, 3- energy level schemes, $l_{am}$ is the length of AM. $\tau_r = \frac{2l_c}{c}$ is the round trip transit time, $l_c$ is the cavity optical length. while c is the speed of light in vacuum. $K_{sgi(i=1,2)} = \frac{2\sigma_{sgi}L_{sa}}{\tau_r}$ is the coupling coefficient between $\varphi_i$ photons and the ground state ions of SA respectively. $K_{sei(i=1,2)} = \frac{2\sigma_{sei}L_{sa}}{\tau_r}$ is the coupling coefficient between $\varphi_i$ and the excited state ions of SA respectively. $\sigma_{sgi(i=1,2)}$ is the absorption cross sections ($cm^2$ ) of ground state of SA, $\sigma_{sei(i=1,2)}$ is the absorption cross sections ($cm^2$) of excited state of SA, $L_{sa}$ is the length of SA. $\gamma_{ci(i=1,2)} = \left(ln\frac{1}{R_i} + L_i\right)$ is the cavity decay rate represents the sum of losses in $\varphi_i$ because of the reflectivity ($R_i$), absorption and scattering mechanisms in cavity( $L_i$) . $\gamma_{pi(i=1,2)}$ is the reduction population factor equals 1,2 for four and three energy levels schemes of AM system respectively. $n_{gs}, n_{es}$ the ions population (No. of ions density ) of the ground and excited levels of SA respectively. $\tau_g$ the fluorescence life time of the upper laser level ( $^4F_{3/2}$ ), $\tau_{se}$ the life time of the SA. $R_P$ is the pumping rate.

The build-up time of PQS laser pulses in generally very short compared with $\tau_g$ and. Then, it is possible to neglect the terms of pumping rate and spontaneous decay of the upper laser level (term1and term3 in equations 3and 4) during pulse generation. As a result, $\tau_{es}$ is very long comparing to the build-up time of PQS laser pulses. Then, it is possible to neglect the third terms of equation 5 and equation 6.

The initial population inversion density (IPID) between the spectral lines and ($N_{g01}$), $^4F_{3/2}$ and $^4F_{9/2}$ ($N_{g02}$) can be estimated at initial time by boundary conditions, $n_{sg} \approx n_0$ or $n_{se} \approx 0$, where ($n_0 = n_{sg} + n_{se}$) is the total ions of SA. $\frac{d\varphi_i}{dt} \approx 0$ in equation 1and 2 because of $\varphi_i$ is very low in value, then the IPID values $N_{g01}$ , $N_{g02}$ for laser medium can be predicted from Equation1 and Equation 2 respectively, as the following:

$$N_{g0i(i=1,2)} = \frac{K_{gsi}n_0 + \gamma_{ci}}{K_{ami}} \quad (7)$$

The threshold population inversion (TPID) for the four and three levels schemes $N_{th1}, N_{th2}$, respectively can be estimated at time of maximum photons density (when the number of photons inside the optical laser cavity reaches to the peak of pulse) by equations1 and 2. At TPID, most of SA ions population in the excited state ( $n_{es}$) can be considering as $n_{se} \approx n_0$ ($n_{gs} \approx 0$); then it can be considered that $\frac{d\varphi_i}{dt} \approx 0$, to get:

$$N_{thi(i=1,2)} = \frac{K_{sei} n_0 + \gamma_{ci}}{K_{ami}} \quad (8)$$

The pulse energy can be estimated by the expression [15].

$$E_i = \frac{(N_{goi} - N_{gfi})}{N_{goi}} \frac{(N_{goi} - N_{gfi}) h\upsilon_i}{\gamma_i} \quad (9)$$

Where $N_{gf}$ is the final population inversion density (FIPD) that was gotten from computations. The pulse power can be estimated by:

$$P_i \approx -\frac{h\upsilon_i \gamma_{ci}}{\gamma_i} \left[ N_{thi} - N_{goi} - N_{thi} \ln\left(\frac{N_{goi} - N_{thi}}{N_{goi}}\right) \right] \quad (10)$$

The duration of pulse can be estimated by [12]:

$$\tau_i = \frac{E_i}{P_i} \quad (11)$$

## III. RESULTS AND DISCUSSION

The rate equations 1-6 have been solved numerically by Rung-Kutta-Fehellberge methods -. The input data that was used in this simulation reported as shown in Table 1.

Table 1: Parameters for the numerical calculation

| Parameter | Value | Parameter | Value |
|---|---|---|---|
| $\sigma_{a1}$ | 2.7 $\times 10^{-19} cm^2$ [17] | $R_1$ | 0.94 |
| $\sigma_{a2}$ | 1.5 $\times 10^{-20} cm^2$ [17] | $\sigma_{gs1}$ | 7 $\times 10^{-18} cm^2$ [6] |
| $\lambda_1$ | 1.064$\mu m$ [18] | $\sigma_{es1}$ | 2.6 $\times 10^{-18} cm^2$ [6] |
| $\lambda_2$ | 0.946$\mu m$ [18] | $\sigma_{es2}$ | 1.1 $\times 10^{-18} cm^2$ [6] |
| $\sigma_{gs2}$ | 4 $\times 10^{-18} cm^2$ [18] | $\gamma_1$ | 1 [6] |
| $R_2$ | 0.99 | $\gamma_2$ | 2 [6] |

From figures (3-a,b,c,d), it was observed that both pulses released at advance (earlier ) time as the value of $L_{sa}$ increases, the passive Q-switching for $\lambda = 1.064nm$, $\lambda = 0.946nm$ released respectively at time 58ns, 60 ns approximately at $L_{as} = 0.35cm$, while released at time 34 ns ,36 ns respectively approximately at $L_{as} = 0.46cm$. The study explains that because of the increases in the values of initial population inversion density (IPID) of active medium (AM) as shown in the mentioned figures.

Figure 4 shows an increase in the initial values of IPID of the two type schemes of energy levels as a function of $L_{sa}$ , and this behavior is an enhancement of the result of our study in figure 3.Our result showed that the large number of laser photons that were prevented from oscillating inside resonator led to build a high value of population inversion density (PID).

Figure 5 represents the difference between the initial and final values of the population inversion density. It showed an increase in the difference values with an increase in $L_{sa}$ which leads to an increase in the density number of laser photons as shown in figures 3(a,b,c,d).

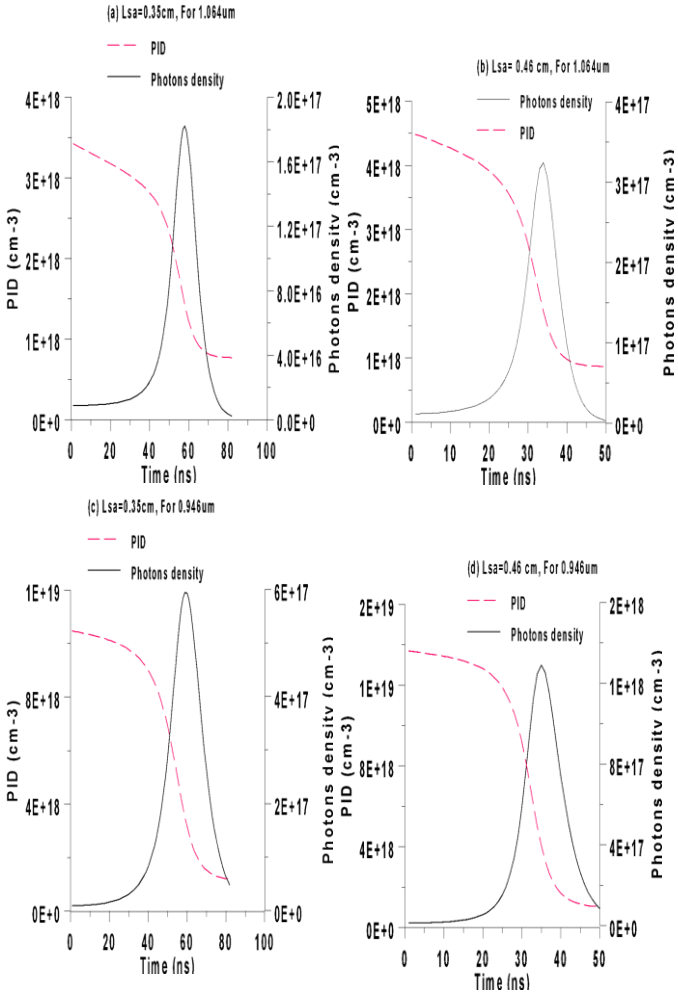


Figure 3: Profiles of PQS inversion density as a function of $L_{as}$ , (a,b for 4-levels scheme, c, d for 3-level scheme of active medium)

Figure 6 shows the decrease in the duration of both pulses as a function of $L_{sa}$ . The duration time of $\lambda = 1.064nm$ and $\lambda = 0.946nm$ pulses approximated to 16.8ns, 14.6 ns respectively at $L_{as} = 0.35cm$ they approximate to 10.8 ns, 9.2 ns respectively at $L_{as} = 0.46cm$ . that might be due to the rapid construction of both pulses, which led to the decreasing in rising and filing times as shown in figures (7,8) respectively

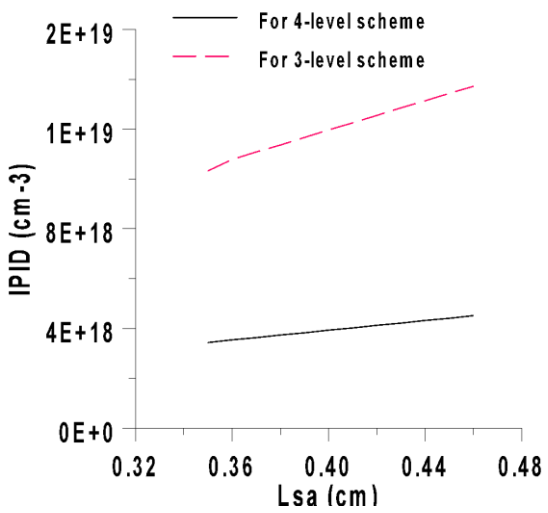


Figure 4: Initial population inversion density as a function of $L_{as}$

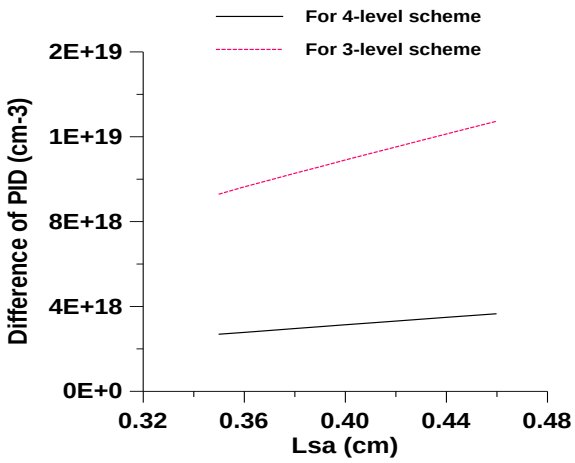


Figure 5: Difference of population inversion density as a function of $L_{sa}$.

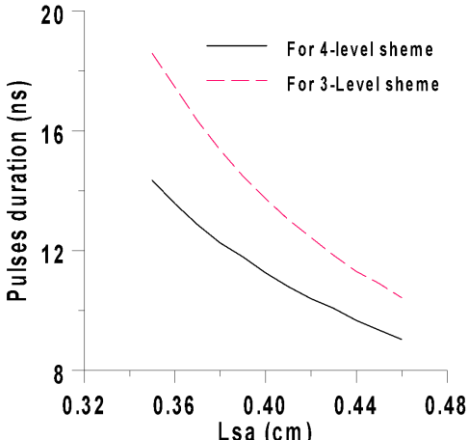


Figure 6: Pulse duration function of $L_{as}$

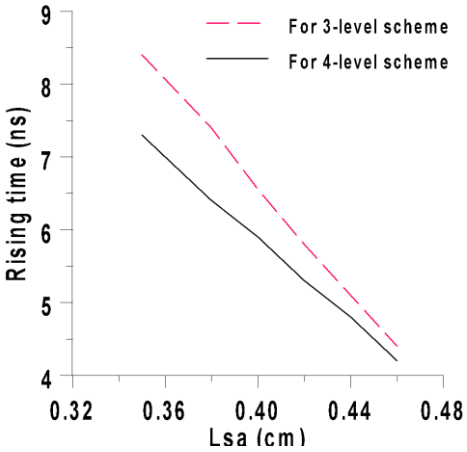


Figure 7: Rising time as a function of

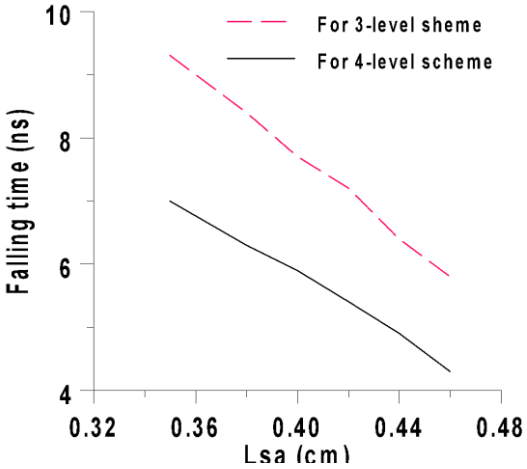


Figure 8: Falling time as a function of

Figure 9 shows the increasing in the energy of both pulses with increasing $L_{sa}$ because of the increasing in the IPID as shown in figure 4, and that resulted in an increase in the maximum value of each pulse's photons as shown in figure10.

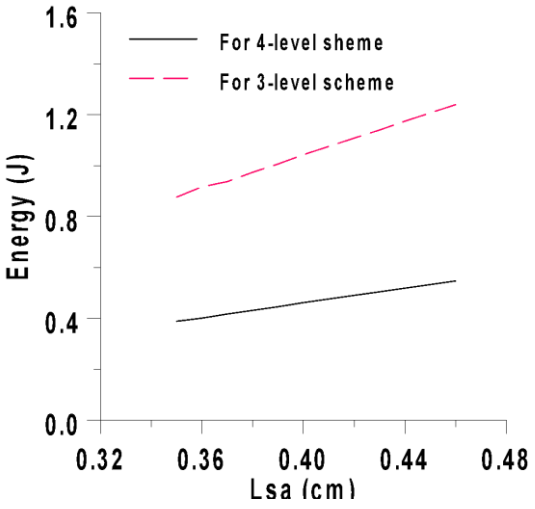


Figure 9: Pulse energy as a function of $L_{as}$

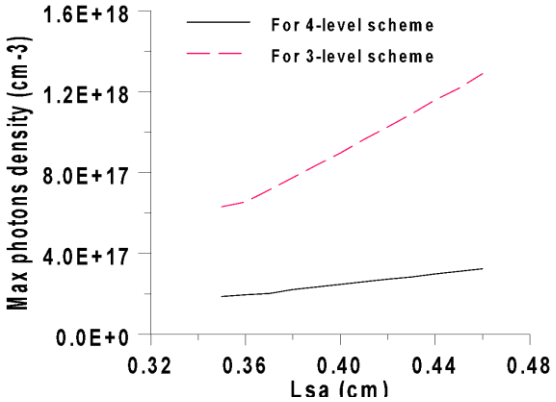


Figure 10: Max. of photons density as a function of $L_{as}$

Figure 11 shows the increased value of each pulse's power by increasing $L_{sa}$. The power of $\lambda = 1.064\,\mu m$ and $\lambda = 0.946\,\mu m$ pulses approximated to $4.7\times10^{7} Watt$ and $2.8\times10^{7} Watt$ respectively at $L_{as} = 0.35cm$, while they approximated to $1.18\times10^{8} Watt$ and $5.8\times10^{7} Watt$ respectively at $L_{as} = 0.46cm$ .this can be explained because of increased energy and decreased duration time of both pulses as shown in Figure 9 and Figure 6 respectively.

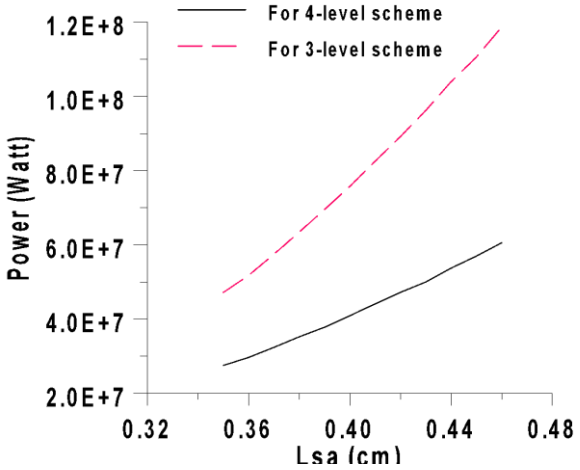


Figure11: power as a function of $L_{as}$

## IV. CONCLUSIONS

The $Nd^{+3}$:YAG dual passive Q-switching ($\lambda = 1.064\ um\ and\ \lambda = 0.946\ um$) are release at earlier time with accompanied by short rising and falling times caused short duration time when the Lsa increase. It is also the dual pulses characterized by increase the energy and the power with the increase the value of Lsa. Therefore, it can be concluded from the results that increasing the length of the saturable absorber lead to impulse the characteristics of dual laser pulses of passive Q-switching.

CONFLICT OF INTEREST `

Authors declare that they have no conflict of interest.

## REFERENCES


[1]. Y. Shen, X. Fu, C.Yao ,W. Li , Y.Wang, X.Zhao , Y.Ning. " Optical Crystals for 1.3 μm All-Solid-State Passively Q-Switched Laser". *Crystals.* 29;12(8):1060. Jul 2022.

[2] X.Zhang , K.Zhong , H.Qiao, Y. Zheng, F.Li, D.Xu, J.Yao. "A passively Q-switched dual-wavelength laser with pulsed LD coaxial end-pumped configuration". *InAdvanced Lasers, High-Power Lasers, and Applications* XIII (Vol. 12310, pp. 24-30). SPIE. Dec 28, 2022.

[3]. Z.Ali , Z.Abdulsada , N.Arasavalli, S.Kadhim, & H. Akram "Initial Transmission Influence on Saturable Absorber Absorption Activity of Passive Q-Switching Erbium-Doped Fiber Laser System". *University of Thi-Qar Journal of Science*, *10*(2), 224-229. (2023).

[4]. M.Li , Y.Qin, C.Wang , X.Liu , S.Long, X.Tang , T.Wen. "Nonuniform pumped passively Q-switched laser using Nd: YAG/$Cr^{+4}$: YAG composite crystal with high-pulse energy". *Optical Engineering*. 1;58(3):036106-. Mar 2019.

[5]. H.Tanaka , C.Kränkel, F.Kannari . "Transition-metal-doped saturable absorbers for passive Q-switching of visible lasers". *Optical Materials Express*. 1;10(8):1827-42. Aug 2020.

[6]. W.Koechner. Solid-state laser engineering. Springer; Nov 11, 2013.

[7] R.Yan , Y.Zhou, X.Li, Y.Liu, Y.Jiang, W.Yao, F.Peng, Q.Zhang, R.Dou, J.Gao. "$^4F_{3/2}\rightarrow\ ^4I_{9/2}$ and $^4F_{3/2}\rightarrow\ ^4I_{13/2}$ laser operations with a Nd: GdTaO4 crystal". *Optics & Laser Technology*. 1;131:106444. Nov 2020.

[8] MA. Mahmood, SR.Mahdi. "Numerical Analysis of a Lasing Output for the Quasi _ Three _ Level Thin Disk Lasers". InJournal of Physics: *Conference Series*. 2021 May 1 (Vol. 1879, No. 3, p. 032116). IOP Publishing. May 2021.

[9] Chen F, Sun J, Yan R, Yu X. "Reabsorption cross section of Nd3+-doped quasi-three-level lasers". *Scientific reports*. 4;9(1):5620. Apr 2019.

[10] Ma C, Zhu J, Hu Z, Wen Z, Long J, Yuan X, Cao Y. Spectroscopic Properties and Continuous Wave Laser Performances at 1064 nm of Nd3+: LuAG Transparent Ceramic. *IEEE Photonics Journal*. 15;9(2):1-4. Mar 2017

[11] A.Sara, M. Abdul kareem."Rate Equations Model to Simulate the Dual Generation of $Nd^{+3}$: YAG Passive Q-swiched Laser Pulses", *Indian Journal of Science and Technology*, 27-10-: 3462-3470. (40)2023. https://doi.org/ 10.17485/IJST/v16i40.1748

[12] S. Bassem Kadhem and A. Mahdi Salih," Simulation of Raman spontaneous scattering factor effect on Stoke Raman and passive Q-switching pulses characteristic", *IOP Conference Series: Materials Science and Engineering*, 928,doi:10.1088/1757-899X/928/7/072160. 2020.

[13] K. Semwal, SC .Bhatt. "Study of Nd3+ ion as a dopant in YAG and glass laser". *International Journal of Physics*. 1(1):15-21. 2013.

[14] Ö. GÜREL. Master of Science Thesis Stockholm, *Sweden* 2009.